Effect of Cross-Winds to Apparent Flame Height and Tilt Angle from Several Kinds of Fire Source

Yasushi OKA[1)], Osami SUGAWA[!2)], Tomohiko IMAMURA[3)] and Yoshiyuki MATSUBARA[4)]

1) Department of Safety Engineering, Yokohama National University
79-5 Tokiwadai, Hodogaya-ku, Yokohama 240-8501, Japan
2) Center for Fire Science and Technology, Tokyo University of Science
2641 Yamasaki, Noda, 278-8510, Japan
3) Graduate school, Department of Safety Engineering
Yokohama National University
4) National Research Institute of Fire and Disaster
14-1 Nakahara 3 Chome, Mitaka, Tokyo, 181-8633, Japan

ABSTRACT

Experiments with a single fire source were carried out in an unconfined space to characterise the effects of cross-winds on apparent flame heights and flame tilt angles. Three sets of propane burners were used as model fire sources. One was a small circular burner, the other was large square burners, and the other was rectangular burners, having the aspect ratio ranging from 1 to 6. A refined empirical model on the apparent flame heights of the inclined flames modified by heat release rate and aspect ratio of fire source was presented. We also developed an empirical model of the flame tilt angles based on the balance of mass between the fluxes given by the upward hot current and the cross-winds. These models are correlations with respect to dimensionless heat release rates, Froude numbers and aspect ratios of fire sources. The values of empirical coefficients and exponents of the correlations were derived from the experimental results.
Key words: unconfined fire, cross-wind, apparent flame height, flame tilt, shape of fire source

INTRODUCTION

The research on flame shape and plume property from a single fire source in the presence of cross-winds in unconfined space was reported by Thomas [1], AGA [2] and other researchers [3-5]. Oka and Sugawa also have conducted some experiments and proposed the empirical formulae on the apparent flame height and flame tilt angle [6, 7]. These models were derived based on experimental results with a square burner of 0.1 m x 0.1 m and releasing dimensionless heat release rate, Q*, ranging from 0.2 to 4.5. This range of Q* corresponds to the heat release rate from the fire of a wooden house and an upholstered furniture. The lengths of these combustibles also becomes from 0.5 m to 15 m. However, the ranges of Q* and the representative lengths correspond to urban fires become from 0.01 to 0.05 and from 30 m to 100 m, respectively.

[!] One of the authors (O.S.) has recently moved following address.
Faculty of Systems Engineering, Department of Mechanics Design, Tokyo University of Science, Suwa 5000-1Toyohira, Chino, 391-0292, Nagano, Japan

The main objective of the current work is to investigate the possibility of applying the empirical formulae developed in the past on the apparent flame heights and the flame tilt angles to the situation of urban fires, namely in the range of small Q*. In addition, we examined how the aspect ratio of rectangular fire sources affects these parameters.

Definition of the apparent flame height and the flame tilt

In this study, the flaming region was defined by temperature records and visual observation aided by video images. In the cases that the flaming region has defined by temperature, the accuracy of the variables that represent the flame properties depends strongly on the temperature of the isotherm used to delineate the flame. Figure 1 shows a comparison between flaming regions given by a digital camera (FinePix6900Z, FUJIFILM) and isotherm curves. The flaming region given by a 35mm camera corresponds approximately to ΔT =200 - 300K. Thus ΔT =250K is employed to define the flaming region. The values for the apparent flame height and the inclined flame angle were taken from the isotherm curves and video images. These isotherm curves were constructed using measured temperatures in parallel to the cross-wind direction along the centreline of the fire source.

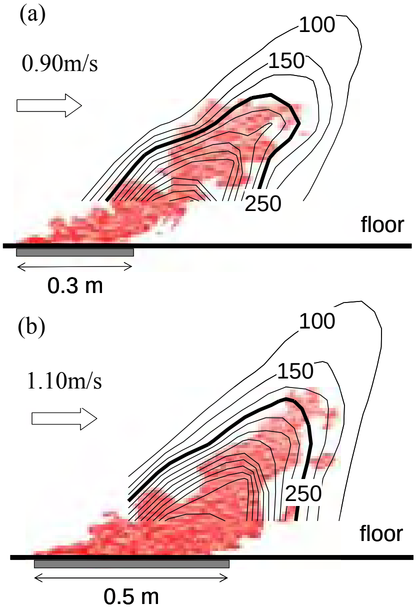

Figure 1 Comparison between isotherm and digital camera image. (a) Ap=3 (0.1m ×0.3m burner), (b) Ap=5 (0.1m×0.3m burner), Q=30kW

The apparent flame height was defined as the vertical length from the intersection of the isotherm curve of $\Delta T = 250$ K and the flame axis to burner surface level. The second set of the apparent flame heights and tilt angles were obtained from video images (Sony, DCR-PC120), namely as the vertical length from the front of continuous or intermittent flames to the burner surface level. These data were obtained from arbitrary successive 60 frames (for 2 seconds in every 1/30 second) and defined as having the 50% appearance probability.

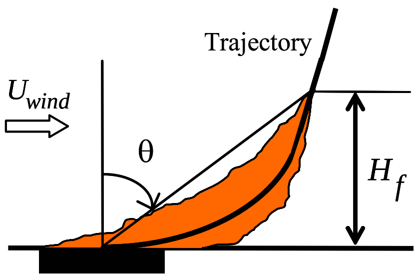

Figure 2 Definition of apparent flame height and flame tilt angle.

The tilt angle, θ, is defined by the angle formed by the straight line between the centre of the burner surface and the intersection of the flame axis and the front of the isotherm curve of $\Delta T = 250$ K. This tilt angle was measured from the vertical. Definition of these parameters is shown in Figure 2.

EXPERIMENTAL PROCEDURES

Three sets of tests, TEST I, II, and III, were conducted in this study. TEST I was carried out as basic experiment for examining the effect of the cross-winds for flame shape and these data were used for developing the empirical formula on an apparent flame height and flame tilt angle. TEST II was carried out in order to examine the effect of fire source shape for the apparent flame height. TEST III was also conducted in the range of small value of Q* and these data were used to enlarge the application range of the empirical formula on the apparent flame height, which was developed using the experimental data of TEST I. In all the experiments described in the following, the propane gas was used as a fuel. The surface of the fire source was placed at the same level of the artificial floor. The values for temperatures were averaged for last 3 minutes, one of a 10 minute test, this duration being assumed to be at a quasi steady state for both heat release rate and cross-wind velocity.

<u>Outline of test equipments</u>

TEST I

Figure 3 shows a schematic diagram of the experimental apparatus employed in TEST I. The burner, ventilation duct and an artificial floor (1.2 m wide and 1.8 m long) were set 0.92 m above the floor of the experimental facility. The centre of the porous gas burner with a diameter of 0.2 m was positioned at 0.9 m from the ventilation duct, which coincided with the centreline of the cross-wind. The heat release rate was varied in four stages as 7.5, 15.0, 22.5 and 30.0 kW. This heat release rate corresponds to fires ranging from 0.38 to 1.50 for Q*. A cross-wind was supplied from the rectangular duct, whose dimension was 1.2m x 1.2m, which is connected to the fan via a honeycomb filter. The velocity was varied in four stages as 0.55, 1.11, 1.66 and 2.20 m/s that correspond to the Fr of 0.15 to 2.47.

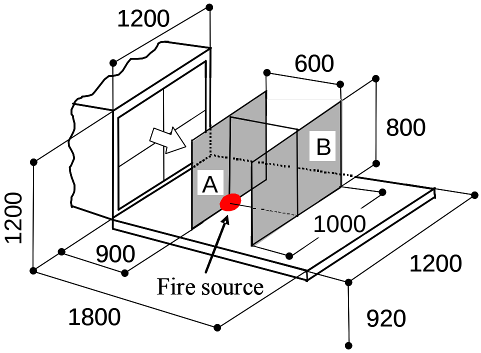

Figure 3 Schematic diagram of experimental apparatus in TEST I & II. Unit:mm

TEST II

To understand the effects of aspect ratio of burner on the apparent flame heights and flame tilt angles, we employed rectangular burners of which their aspect ratio varied from 1 to 6. The rectangular burner was placed in such a way that its short side faced the cross-winds. Two sets of heat release rates were adopted. One was a constant heat release rate of 45 kW regardless of the aspect ratio. The other was a constant heat release rate per unit area of the burner surface. These heat release rates correspond to fires ranging from 2.13 to 12.75 for Q^*_{rec}. Velocities of the cross-winds were changed in four stages as 0.55, 0.90, 1.11 and 1.66 m/s that correspond to the Fr of 0.31 to 2.81.

TEST III

A series of tests were carried out at FRI. Burner and artificial floor was set on the stage which was placed front of the outlet of cross-winds and its dimension was 5.4m(W) x 7.2m(L) in the full scale experimental facility, whose dimension was 25.2m(W) x 24.5m(L) x 20.0m(H), as shown in Figure 4. The dimension of this artificial floor was

4m(L) x 3m(W) x 0.5m(H). Two kinds of square porous burners, the dimensions of which were 1m x 1m and 0.5m x 0.5m. were employed. The centre of these burners were placed at 7.54 m from the outlet of cross-winds and matched to the centreline of the cross-winds. The heat release rate was varied in four stages as 60, 75, 120 and 180 kW. These heat release rates correspond to fires ranging from 0.05 to 0.38 for Q*. A stabilised cross-wind was supplied through the opening with a diameter of 4m, which was installed at the centre of the sidewall and was connected to the fan through the several filters. The velocity was varied in 5 stages as 0.56, 0.80, 1.20, 1.60 and 2.79 m/s that correspond to the value of 0.032 to 0.79 for Fr.

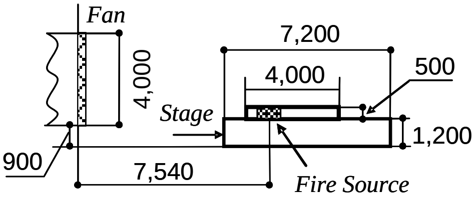

Figure 4 Schematic diagram of experimental apparatus in TEST III. Unit:mm

Temperature measurements

TEST I

The temperature field constructed by inclined fire plume was measured using K-type thermocouples with a diameter of 0.65 mm. As shown in Figure 3, these thermocouples were installed in the plane of A and B of H-shape wire network consisted of stainless steel wire with 2 mm diameter, whose dimension was 1.0m(W) x 0.6m(L) x 0.8m(H). Fifty points of thermocouples were installed in each plane with the interval of 0.1 m. The staggered arrangement of the thermocouple position was employed in parallel between the planes to avoid overlap. These thermocouples were also placed at staggered arrangement in perpendicular to the direction of cross-wind in each plane. The thermocouples were also installed in the central axis of both planes. The H-shape wire network was moved 5 times with its datum set along the centre of the burner in every 0.1 m to the downwind in one test. The first position at 0.5 m from the ventilation duct is to be the standard position for plane A. The data was obtained in every position. Therefore, the measured region was 1.0m(W) x 1.2m(L) x 0.8m(H).

TEST II

No measurements for temperature were done in TEST II.

TEST III

Temperatures were measured using K-type thermocouples with a diameter of 0.32 mm. These thermocouples were installed in plane-shape wire network consisted of stainless wire with 2 mm diameter, whose dimension was 0.4m(L) x 1.2m(H), with the interval of 0.1 m. This plane-shape network was moved 6 times with its datum set along the centre of the burner in every 0.5 m to the downwind in one test. The data was obtained in every position. Therefore, the measured region was 2.8m(L) x 1.2m(H). The position in the 0.1 m upwind from the upwind rim of the fire source was defined to be the control position.

Experimental conditions

The experimental conditions in each test were listed in Table 1. The values of cross-wind mean the average velocities and these were obtained by dividing the total volumetric flow by the effective area, as shown in equation (1).

$$U_{wind} = \sum_{i=1}^{n} s_i v_i \Big/ \sum_{i=1}^{n} s_i \qquad (1)$$

The heat release rates also mean the values assuming the complete combustion.

Table 1 Experimental conditions in each test

TEST I Q^*=0.375 - 1.50

	0.55 m/s	1.11 m/s	1.66 m/s	2.20 m/s
7.5 kW	O	O	O	O
15.0 kW	O	O	O	O
22.5 kW	O	O	O	O
30. kW	O	O	O	O

TEST II Q^*_{rec} = 2.13 - 12.75

Aspect ratio	HRR (kW)	average velocity (m/s)
Ap=1	7.5, 45.0	0.55, 0.90, 1.11, 1.66
Ap=2	15.0, 45.0	0.55, 0.90, 1.11, 1.66
Ap=3	22.5, 45.0	0.55, 0.90, 1.11, 1.66
Ap=4	30.0, 45.0	0.55, 0.90, 1.11, 1.66
Ap=5	37.5, 45.0	0.55, 0.90, 1.11, 1.66
Ap=6	45.0	0.55, 0.90, 1.11, 1.66

TEST III Q^*=0.05 - 0.38

	0.56 m/s	0.80 m/s	1.20 m/s	1.60 m/s	2.79 m/s
60 kW	O				
75 kW	●				
120 kW	O				
180 kW	O	O	O	O	O

O : 1m x 1m fire source, ● : 0.5m x 0.5m fire source

RESULTS & DISCUSSIONS

Cross-wind profile

TEST I & II

Figures 5(a), (b) show the typical horizontal and vertical profiles at 1.0 m downwind from the outlet of the cross-wind with the different frequency in the absence of a flame. Figure 5(a) shows the horizontal profile in perpendicular to the wind direction at 0.45 m height from the artificial floor. It is considered that horizontal profile shows almost uniform in both regions within 0.40 m from the centre. The similar tendency was confirmed at another height and at other different downwind position. Figure 5(b) shows the vertical profile in parallel to the wind direction. The velocity gradually increased up to 0.45 m above the artificial floor level and became approximately uniform in the region over 0.45 m high. The value of the power for the velocity profile with height varies from 1/8 to 1/7, depending on the experimental condition for the cross-winds. This relation corresponds to that in flat open country [9].

TEST III

Figures 6(a), (b) show the typical horizontal and vertical wind profiles at 7.54 m downwind from the outlet of the cross-wind, namely at the centre of fire source, with the different velocity at the situation without a flame. Figure 6(a) shows the horizontal profile in perpendicular to the wind direction at 0.65 m height from the artificial floor. It is considered that horizontal profile shows almost uniform within the measured region. Figure 6(b) shows the vertical profile in parallel to the wind direction on the centre of fire source. Although there are some fluctuations in vertical profile according to increasing the velocity of cross-wind, it is considered that vertical profile almost shows flat.

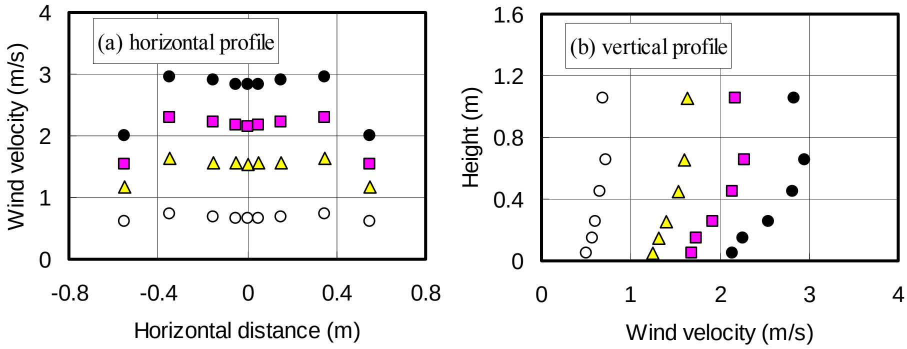

Figure 5 Typical wind profile at 1.0m downwind from the ventilation duct in TEST I and II. (a) horizontal profile at z=0.45m (b) vertical profile

○ frequency of 15Hz △ frequency of 30Hz ■ frequency of 40Hz ● frequency of 50Hz

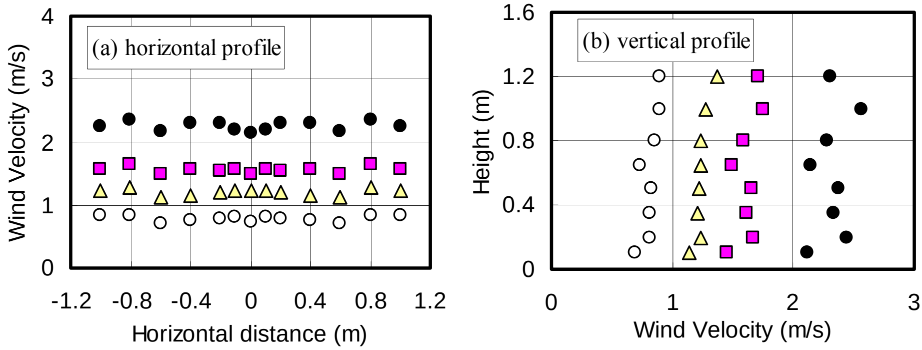

Figure 6 Typical wind profile at the centre ot fire source in TEST III. (a) horizontal profile at z=0.65m (b) vertical profile along the centreline of fire source

○ 0.82 m/sec △ 1.26 m/sec ■ 1.66 m/sec ● 2.41 m/sec

<u>The apparent flame height</u>

The flame height in the absence of cross-winds has been measured by various techniques, such as a video recording, a 35mm photo, an infrared camera, and thermocouples and various empirical formulae have been reported as a function of heat release rate [10-14]. In this study, the concept of the apparent flame height was introduced in order to represent the height of the inclined flame in the presence of cross-winds. The data on the apparent flame heights and inclined flame angles obtained in these experiments were listed in Table 2.

We examined how the difference of reading method influences the apparent flame height. In other words, the flame heights read from the isotherm curves were compared with those from video images. Two kinds of flame height defined by the continuous and

Table 2 The list of experimental results.

TEST I

HRR (kW)	Uwind (m/s)	θ_1 (degree)	θ_2 (degree)	Hf_1 (m)	Hf_2 (m)	Hf_3 (m)
7.5	0.55	45.3	29.4	0.23	0.28	0.37
7.5	1.11	68.7	41.3	0.13	0.21	0.30
7.5	1.66	77.0	51.3	0.10	0.21	0.21
7.5	2.20	80.5	54.0	0.05	0.18	0.19
15.0	0.55	34.9	22.1	0.43	0.41	0.46
15.0	1.11	59.3	43.6	0.24	0.32	0.39
15.0	1.66	74.4	53.2	0.14	0.27	0.34
15.0	2.20	78.6	59.7	0.13	0.21	0.28
22.5	0.55	35.1	21.3	0.51	0.47	0.61
22.5	1.11	60.2	42.5	0.31	0.35	0.44
22.5	1.66	69.8	54.8	0.24	0.30	0.35
22.5	2.20	79.8	60.6	0.12	0.24	0.34
30.0	0.55	32.4	25.6	0.61	0.44	0.69
30.0	1.11	58.6	46.7	0.38	0.35	0.48
30.0	1.66	68.5	50.8	0.29	0.33	0.41
30.0	2.20	79.3	60.9	0.15	0.29	0.35

TEST II

	HRR (kW)	Uwind (m/s)	θ_2 (degree)	Hf_2 (m)		HRR (kW)	Uwind (m/s)	θ_2 (degree)	Hf_2 (m)
Ap=1	45.0	0.55	28.4	0.65	Ap=4	45.0	0.55	30.9	0.60
	45.0	0.90	40.2	0.53		45.0	0.90	46.9	0.50
	45.0	1.11	50.5	0.47		45.0	1.11	55.4	0.39
	45.0	1.66	62.5	0.32		45.0	1.66	62.5	0.33
	7.5	0.55	50.4	0.24		30.0	0.55	36.7	0.46
	7.5	0.90	54.7	0.22		30.0	0.90	50.9	0.36
	7.5	1.11	59.5	0.18		30.0	1.11	57.0	0.32
	7.5	1.66	65.3	0.16		30.0	1.66	65.2	0.27
Ap=2	45.0	0.55	32.0	0.68	Ap=5	45.0	0.55	20.0	0.59
	45.0	0.90	45.0	0.54		45.0	0.90	44.8	0.49
	45.0	1.11	54.9	0.44		45.0	1.11	56.3	0.38
	45.0	1.66	64.9	0.31		45.0	1.66	64.4	0.34
	15.0	0.55	48.0	0.32		37.5	0.55	33.5	0.46
	15.0	0.90	53.2	0.30		37.5	0.90	44.2	0.39
	15.0	1.11	58.0	0.25		37.5	1.11	51.3	0.35
	15.0	1.66	64.8	0.21		37.5	1.66	57.0	0.33
Ap=3	45.0	0.55	26.4	0.71	Ap=6	45.0	0.55	27.8	0.58
	45.0	0.90	42.6	0.56		45.0	0.90	38.3	0.50
	45.0	1.11	54.7	0.44		45.0	1.11	51.4	0.37
	45.0	1.66	64.0	0.33		45.0	1.66	58.5	0.33
	22.5	0.55	36.3	0.48					
	22.5	0.90	53.5	0.34					
	22.5	1.11	57.5	0.29					
	22.5	1.66	65.1	0.24					

TEST III

HRR (kW)	Uwind (m/s)	θ_1 (degree)	θ_2 (degree)	Hf_1 (m)	Hf_2 (m)
120.0	0.56	82.0	50.6	0.11	0.35
60.0	0.56	84.1	65.4	0.07	0.20
180.0	0.56	75.1	47.4	0.25	0.52
180.0	0.80	82.1	-----	0.15	-----
180.0	1.20	82.0	-----	0.15	-----
180.0	1.60	82.4	-----	0.14	-----
180.0	2.79	84.0	76.2	0.07	0.21
75.0	0.56	68.8	55.5	0.28	0.43

θ_1 isotherm curve of 250 K, θ_2 VTR
Hf_1 isotherm curve of 250 K, Hf_2 VTR (continuous)
Hf_3 VTR (intermittent)

intermittent height of the inclined flame were read from the video images. And, three kinds of flame height defined by the isotherm curve of ΔT = 100K, 250K, and 450K were read from the isotherm. These results used in this comparison were obtained in the experiment of TEST I and were plotted against the combination function of Q* and Fr as shown in Figure 7. The apparent flame height defined by the isotherm curves were varied their intercepts according to the temperature rise for delineating the flaming region. But the value of power, which means the dependence to the function of Fr and Q*, was maintained the value of –3/4. However, the results obtained from video images show the dependence of –2/5 power to the function of Fr and Q* and this relation was kept for the apparent flame height defined as both continuous and intermittent flames. When the above-mentioned results are brought together, the relationship between the apparent flame height and the combination function of Q* and Fr can be represented in equation (2).

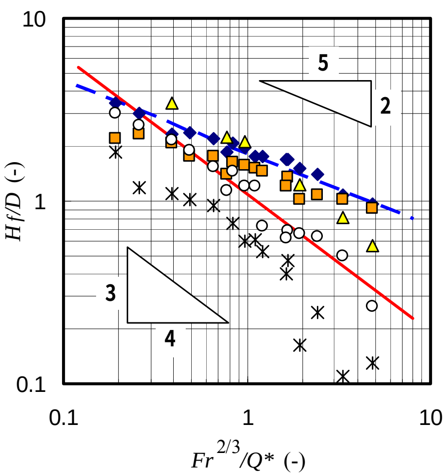

Figure 7 Comparison of apparent flame height given by video images and isotherm curves.

video image (continuous flame)
video image (intermittent flame)
ΔT = 100 K ΔT = 250 K
ΔT = 450 K
Eq. (2) for intermittent flame
Oka et al [16]

$$\frac{H_f}{D} = \alpha \left(\frac{Fr^{2/3}}{Q^*} \right)^{\beta} \quad ; \text{where} \quad 0.2 \le \frac{Fr^{2/3}}{Q^*} \le 5 \tag{2}$$

for isotherm curves of $\Delta T = 250\text{K}$ $\alpha = (1 \pm 0.1)$, $\beta = -3/4$

for VTR images $\alpha = 1.46$, $\beta = -2/5$ (defined by continuous flame)

$\alpha = 1.85$, $\beta = -2/5$ (defined by intermittent flame)

In the presence of the cross-wind, it is considered that heat is carried to the downstream by three kinds of media such as the inclined fire plume, cross-winds and radiation. Temperature measured by the thermocouples is given by the total effect of convection and radiation. On the other hand, video images were made by detecting the light emission from the flame. Therefore, it is considered that the power on the combination function shows the different value. Clearly we have to pay attention to the experimental conditions for which the model is derived prior to its use.

The variations of the apparent flame height based on isotherm curves of $\Delta T = 250\text{K}$ against the combination function of Q* and Fr are shown in Figure 8(a). These data were got in TEST I and III. The effect of the fire source scale is very big and it is not possible to apply the empirical formula described in equation (2) without any modification to the flames formed on the fire source in which the value of Q* is very small.

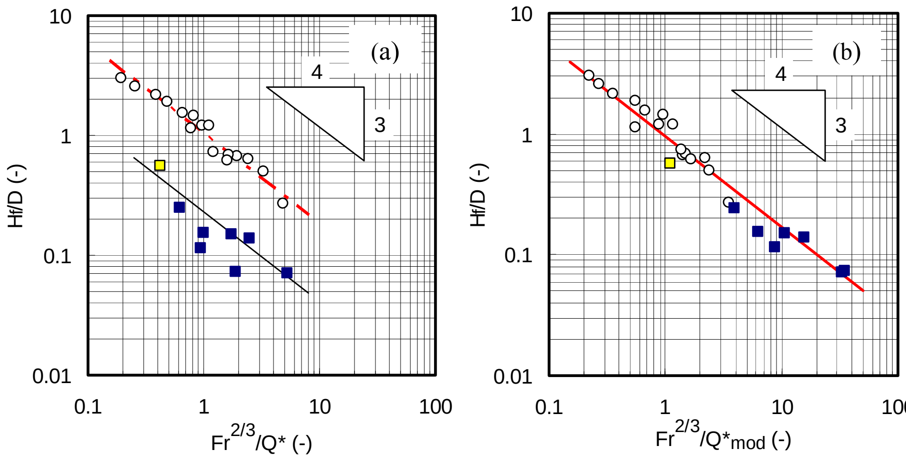

Figure 8 Variation of apparent flame height based on isotherm curves of ΔT =250K against the function of Q* and Fr. (a) before correction. (b) after correction

TEST I ○ ϕ0.2m (Q*=0.38 – 1.50)

TEST III ■ 1m x 1m (Q*=0.05 – 0.16) □ 0.5m x 0.5m (Q*=0.38)

– – – equation (2)

Although the value of both intercept is different, the value of power on the combination function of Q* and Fr shows almost same value. Then the correction was conducted based on following ideas. In unconfined space with the absence of cross-winds, Zukoski [10] has reported the relationship between the flame height and the heat release rate as the value of the heat release rate to be an index. Then, it was assumed that this relation could be inherited even in the presence of cross-winds. In other words, it could be replaced the original Q^* to Q^{*n}, n=2 in the region of $0.05<Q^*<0.38$ and n=2/3 in the region of $0.38<Q^*<12.8$. This modified heat release rate was represented as $Q^*_{mod}=Q^{*n}$. There is a possibility that the range changes by the stacking of further data, because this range was decided on the basis of present experimental results. The data can be matched closely by a line without being dependent on the size of the fire source area, when H_f/D was plotted against the modified function of Q^*_{mod} and Fr as shown in Figure 8(b).

Figure 9(a) shows the variation for the apparent flame height based on video images against the combination function of Q* and Fr. These data were got in TEST I, II and III and defined as the continuous flame height. The fire source scale and shape affect the apparent flame height and it is hard to uniformly represent whole data in equation (2). Moreover, the following features are confirmed from the data of TEST II. In the case of Ap=1, the fire source shape is square, the good coincidence with the empirical formula given in equation (2) can be confirmed. However, the apparent flame heights became large with the increase of the value of Ap. This cause was considered as follows. In this experiment, LPG was employed as the fuel and unburned fuel above the rectangular burner was pushed downstream by the cross-winds and accumulated at the downstream edge of the rectangular burner. Therefore, the uniform combustion reaction does do not progress over the rectangular burner surface, namely the locally active combustion is occurred in the neighbourhood of the downstream edge of the rectangular burner.

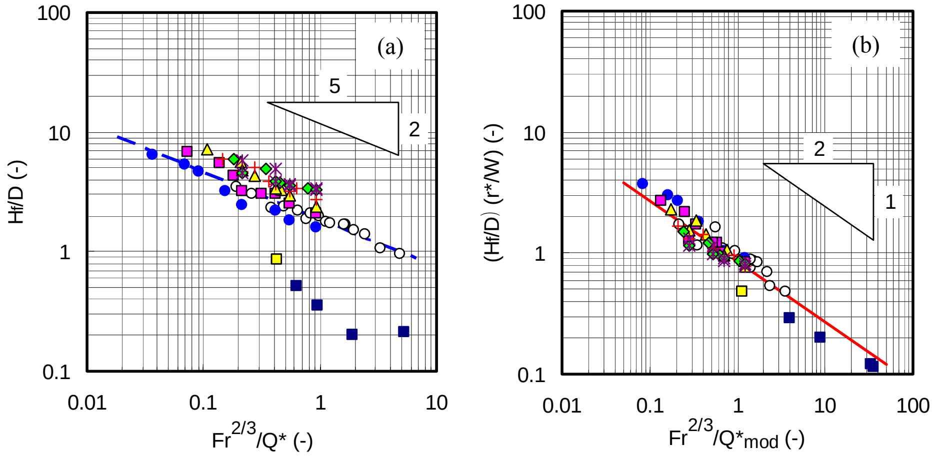

Figure 9 Variation of apparent flame height based on video images against the function of Q* (Q^*_{mod}) and Fr. (a) before correction. (b) after correction

TEST I ○ ϕ0.2m (Q*=0.38 – 1.50)
TEST II ● 0.1m x 0.1m (Q*rec=2.13 – 12.8) ■ 0.1m x 0.2m (Q*rec=2.13 – 6.38)
△ 0.1m x 0.3m (Q*rec=2.13 – 4.25) + 0.1m x 0.4m (Q*rec=2.13 – 3.18)
◆ 0.1m x 0.5m (Q*rec=2.13 – 2.55) ✳ 0.1m x 0.6m (Q*rec=2.13)
TEST III ■ 1m x 1m (Q*=0.05 – 0.16) □ 0.5m x 0.5m (Q*=0.38)
– – – equation (2) —— equation (3)

As mentioned above, the effect of fire source scale could be dealt with by employing the new variable of Q^*_{mod}. The remaining issue is how to take the effect of the burner shape into account. Then we assumed that the flame formed at the downstream edge of the rectangular burner could be regarded as the flame from the circular burner which has the same burning area. The new length of r*, which means the radius of the circular fire source with the area equal to the original rectangular fire source, was introduced. The final formula between the apparent flame height and the combination function of Q^*_{mod} and Fr considering the fire source shape and its scale was given in equation (3) as shown in Figure 9(b). The values of empirical coefficients and exponents of the correlations were derived from the experimental results.

$$\left(\frac{H_f}{D}\right)\left(\frac{r^*}{W}\right)=\alpha\left(\frac{Fr^{2/3}}{Q^*_{\mathrm{mod}}}\right)^{\beta} \tag{3}$$

α=0.50, β= −3/4 (defined by isotherm curve of $\Delta T = 250\mathrm{K}$)
α=0.84, β= −1/2 (defined by video image)

Flame tilt angle

The flame tilt angles got in TEST I, II and III, these data were based on video images, were plotted against the combination function of Fr and Q* shown in Figure 10(a). This combination function was derived assuming that the flame tilt angle was controlled by the balance of the hot current and cross-wind at the average flame height. Namely mass fluxes representing the upward hot current and cross-wind were employed to be the main factors in determining the tilt angle. These are combined with the centreline properties based on upward velocities as proposed by McCaffrey in calm conditions [15], by assuming that the relationship between the distance from the burner surface and centreline upward velocity was inherited although the values of coefficient and power were different. The details of the derivation process have been described in Ref. [7].

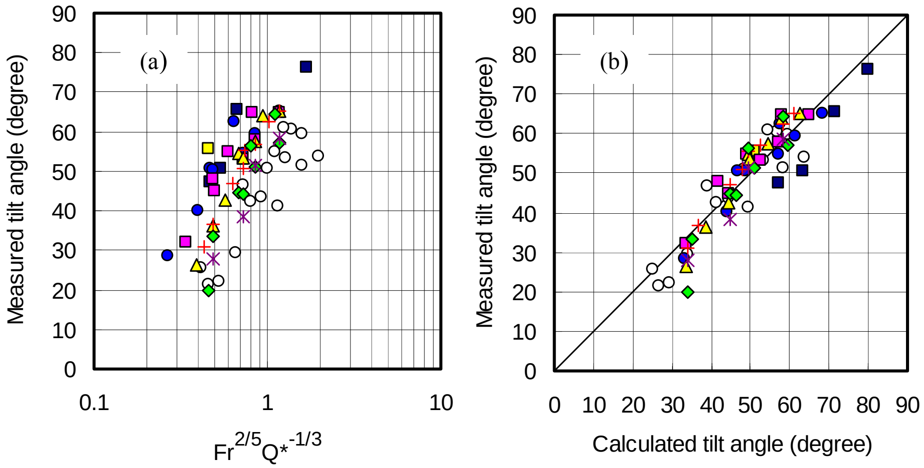

Figure 10 Comparison between predicted and measured tilt angle.
(a) before modification (b) after modification

TEST I ○ ϕ0.2m (Q*=0.38 – 1.50)
TEST II ● 0.1m x 0.1m (Q*rec=2.13 – 12.8) ■ 0.1m x 0.2m (Q*rec=2.13 – 6.38)
△ 0.1m x 0.3m (Q*rec=2.13 – 4.25) + 0.1m x 0.4m (Q*rec=2.13 – 3.18)
◆ 0.1m x 0.5m (Q*rec=2.13 – 2.55) ✳ 0.1m x 0.6m (Q*rec=2.13)
TEST III ■ 1m x 1m (Q*=0.05 – 0.16) □ 0.5m x 0.5m (Q*=0.38)

As shown in Figure 10(a), it is found that a certain relation between the measured flame tilt angle and the function of Fr and Q* was preserved regardless of the shape and scale of the fire source. Therefore, the similar idea employed in developing the model on the apparent flame height was applied to the model for the flame tilt angle. The final formula for predicting the flame tilt angle using Q*, Fr and r* is given in equation (4).

$$\tan\theta = 2.73 Fr^{\frac{2}{5}} \cdot Q^{*-\frac{1}{10}(1+\frac{5}{2}n)} \cdot \left(\frac{W}{r*}\right)^{-\frac{1}{2}}; \qquad \text{where } \; 20^{o} \le \theta \le 80^{o} \qquad (4)$$

where n=2 in the region of 0.05<Q*<0.38 and n=2/3 in the region of 0.38<Q*<12.8. Moreover, it is note that the term (W/r*) should be replaced to (W/r*)π in the case of predicting the tilt angle of flame from the circular burner. Final results obtained using equations (4) are plotted in Figure 10(b). The models may be applied over a wide range and it may be considered that this range covers the practical range.

CONCLUSIONS

The dependence of the apparent flame height against the function of Fr and Q* is different according to the method how the data was defined, such as by isotherm curves or by video images in the presence of cross-wind and value of exponent becomes –3/4 and –2/5, respectively.

Dimensionless formula for the apparent flame height of an inclined flame under the influence of cross-wind has been developed based on the modified dimensionless heat release rate, Froude number and characteristic length of burner. This empirical formula is applicable to the Q* and/or Q^*_{rec} of 0.05 to 12.75 without being dependent on the fire source shape such as square, circle and rectangle.

New formula has been developed to predict the flame tilt angle considering the burner shape. This model is derived from the balance of mass fluxes of wind and hot current, combined with centreline properties of a fire plume.

NOMENCLATURE

A_p : aspect ratio of rectangular burner (-)

C_p : Specific heat at constant pressure ($kJ \cdot kg^{-1} \cdot K^{-1}$)

D : representative length of circular and/or square burner / short side length of rectangular burner (m)

g : acceleration due to gravity (m/s^2)

H_f : apparent flame height (m)

L_{fw} : length of inclined flame (m)

Q : heat release rate (kW)

r* : equivalent length of burner ($= \sqrt{\text{burner area}/\pi}$) (m)

s_i : unit area (m^2)

U_{wind} : representative cross-wind velocity (m/s)

v_i : velocity through the small area i (m/sec)

W : long side length of rectangular burner (m)

ΔT : excess temperature from ambient (K)

ρ_a : density of ambient air (kg/m^3)

θ : the angle formed by the straight line between the centre of the burner surface and the intersection of the flame axis and the front of the isotherm curve of ΔT =250 K (degree)

$Fr = U_{wind}^2/(gD)$ (-)

$Q^* = Q/(\rho_a C_p T_a g^{1/2} D^{5/2})$ (-)

$Q^{*}_{rec} = Q/(\rho_a C_p T_a g^{1/2} W D^{3/2})$ (-)

REFERENCES

1) Thomas, P.H., “The Size of Flames from Natural Fires”, 9th International Combustion Symposium, Combustion Institute, pp.844-859, 1963.
2) American Gas Association, Report IS 3-1, (1974)
3) Yokoi, S., “Temperature Distribution Downwind of the Line Heat Source”, Bulletin of The Fire Prevention Society of Japan, Vol.13, No.2 1965, in Japanese
4) Saga, T., Bulletin of Tohoku Institute of Technology, No. 1, 1996, in Japanese
5) Weise, D.R., and Biging, G.S., “Effects of Wind velocity and Slope of Flame Properties”, Can. J. For. Res. Vol.26, pp.1849-1858, 1996
6) Oka, Y., Kurioka, H., Satoh, H., and Sugawa, O.: “Theoretical Approach on Flame Tilt based on Apparent Flame Heights in Free Boundaries”, Journal of Constr. Engng, AIJ, No.520, pp.147-154, 1999, in Japanese
7) Oka, Y., Kurioka, H., Satoh, H., and Sugawa, O., “Modelling of Unconfined Flame Tilt in Cross-Winds” Int. Assoc. of Fire Safety and Science, Proceedings of the 6th Int. Symposium on Fire, pp.1101-1112, 2000.
8) Sugawa,O., Satoh,H., and Oka,Y., “Flame Height from Rectangular Fire Sources considering Mixing Factor", Int. Assoc. of Fire Safety and Science, Proceedings of the Third Int. Symposium on Fire, pp.435-444, 1991.
9) Davenport, A.G., “The relationship of wind structure to wind loading”, Proc. 1st Int. Conf. on Wind Effects on Buildings and Structures, pp.53-111, 1965.
10) Zukoski, E.E., Kubota, T., and Cetegen, B., “Entrainment in fire plumes”, Fire Safety Journal, vol.3, pp.107-121, 1981a.
11) Hasemi, Y. and Tokunaga, T., “Flame Geometry Effects on the Buoyant Plumes from Turbulent Diffusion Flames”, Fire Science and Technology, Vol.4, No.1, pp.15-26, 1984.
12) Cox, G. and Chitty, R., “some Source-Dependent Effects of Unbounded Fires”, Combustion and Flame, vol.60, pp,219-232, 1985.
13) Heskestad, G., “Peak Gas Velocities and Flame Height of Buoyancy-Controlled Turbulent Diffusion Flames”, 18th Symposium (International) on Combustion, pp.951-960, 1981.
14) Delichatsios, M.A., “Air Entrainment into Buoyant Jet Flames and Pool Fires”, Combustion and Flame, vol.70, pp,33-36, 1987.
15) McCaffrey, B.J., “Purely Buoyant Diffusion Flames ―Some Experimental Results―”, NBSIR79-1910, 1979.
16) Oka, Y., Sugawa, O. and Imamura, T.: “Flame and Temperature Properties from A Single Fire Source in Cross-Winds”, INTERFLAME 2001, Edinburgh, UK, pp.671-681, 2001.

ACKNOWLEDGMENTS

The authors would like to note our sincere thanks to Mr. Yasuaki Okada, undergraduate student of Tokyo University of Science, for his help in carrying out the experiments and also sincere thanks to Professor emeritus Toshisuke Hirano, Dr. Tokiyoshi Yamada and Dr. Daisuke Kohzeki of National Research Institute of Fire and Disaster for their kind supports during the experiments.